

## MiniCal Test Beam Results with APD's \*

J. Cvach

*Institute of Physics, Academy of Sciences of the Czech Republic, Prague, Czech Republic*

We report upon the performance of a small analog calorimeter prototype where scintillating tiles are read out with wavelength-shifting fibers coupled to APDs. This prototype configuration has been tested using a positron beam at DESY with energies between 1–6 GeV. The results for linearity, and energy resolution are in good agreement with our simulation studies and previous measurements using SiPM as photodetector. The present study is a part of an extensive R&D program aimed at the optimisation of a calorimeter for the ILC and it is done in CALICE Collaboration [1].

### 1. INTRODUCTION

The physics requirements at the International Linear Collider (ILC) place high demands on calorimetry [2]. In order to achieve a jet-energy resolution of  $30\%/\sqrt{E}$  both electromagnetic showers and neutral hadron showers have to be well identified and measured [3–5]. The essential requirement is high granularity both in the longitudinal and transverse directions. For the electromagnetic calorimeter the presently favoured option is a silicon-tungsten sandwich calorimeter, while for the hadron calorimeter both analog and digital options are pursued [1, 6].

The analog option of the hadron calorimeter consists of a steel-scintillating tile sandwich calorimeter [7]. High granularity is achieved with small scintillating tiles. The light in each tile is collected by a wavelength-shifting fiber coupled to a silicon photomultiplier (SiPM), a newly-developed photodetector [8], or a conventional avalanche photodiode (APD). Here we summarize the performance of a small hadronic calorimeter prototype that is read out with 33 APDs. Detailed description of the setup and of the results is prepared for publication [9].

### 2. THE MINICAL PROTOTYPE FOR APD READOUT

A small sampling calorimeter prototype, called the MiniCal, has been built for R&D studies of high-granularity calorimeter. The structure consists of 28 layers of 2 cm thick stainless-steel plates. The plates are stacked with 0.9 cm gaps into which thin-walled aluminum cassettes are inserted, each housing nine  $5 \times 5$  cm<sup>2</sup> wide and 0.5 cm thick scintillating tiles in a  $3 \times 3$  matrix as shown in Figure 1. We distinguish between tiles with four neighbours, called center tiles, those with three neighbours, called edge tiles, and the remaining with two neighbours, called corner tiles. The scintillator material is BC408 from Bicron. Each tile is wrapped with 3M reflector foil. The amount of material per layer in terms of radiation lengths and interactions lengths is  $1.15 X_0$  and  $0.12 \lambda$ , respectively.

A 60 cm long wavelength-shifting (WLS) fiber (double clad Y11 300 ppm from Kuraray) collects the scintillation light of each tile and transports the wavelength-shifted light to an APD. To optimize the light guide properties of the fiber an air gap is kept between the scintillator and the fiber. In front of the  $3 \times 3$  mm<sup>2</sup> active area of the APD a rubber mask with four holes is used to hold up to three WLS fibers at a fixed place. The fourth hole is used to insert a clear fiber that transports light from a blue LED to monitor the stability of the APD. For a direct comparison with the beam test results from the SiPM setup [10], we read out the center tile of each layer individually, where more than 95% of the energy of an electron shower is deposited. For the four edge tiles and one corner tile fibers of three

---

\*Participating Institutes are DESY (FLC) Hamburg, ITEP, LPI, MEPHI Moscow and Institute of Physics AS CR, Charles University Prague within the CALICE Collaboration.

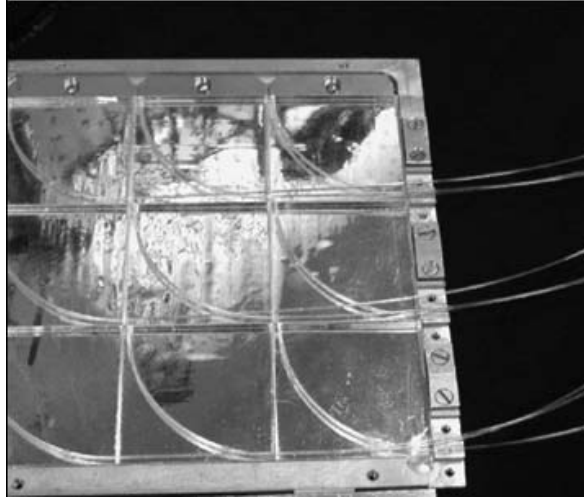


Figure 1: A MiniCal cassette with nine  $5 \times 5 \text{ cm}^2$  scintillating tiles read out by WLS fibers transmitting green light to APDs

consecutive layers are connected to one APD each. A total of twelve layers were equipped in this fashion. Since we have used up all 33 APDs in this way, the remaining three corner tiles are not read out.

The MiniCal is mounted inside an electrically shielded light-tight box. On one side of the MiniCal box three PCB's are mounted holding sockets for electronics, power supplies and cable connections. The four nine-channel preamplifier units are attached here. The APDs are coupled directly to the preamplifiers grouping them in four arrays holding nine detectors each. The temperature inside the box is monitored by three temperature sensors that are read out by a slow control system independently from data taking.

## 2.1. APDs and Preamplifiers

The APDs used were Hamamatsu S8664-55 spl, a special delivery of 33 pieces for our tests with an active surface of  $3 \times 3 \text{ mm}^2$ . Their I-U and C-U characteristics were measured at CERN using the setup of the CMS experiment. The measured I-U dependence [11] was used to sort them into groups of nine with similar gain. At a bias voltage of 420 V, the APD gain was about 250 at a temperature of  $25^\circ \text{C}$ . At this gain the sensitivity of the output signal on temperature and bias voltage is still manageable.

The APD signals were amplified using two types of single channel preamplifiers: a charge-sensitive preamplifier chip from Minsk and a voltage-sensitive preamplifier from Prague built from discrete components. Both preamplifiers typically operate at gains of  $2 \times 10^3 - 10^4$ . The Minsk preamplifier is superior to the Prague preamplifier with respect to the signal-to-noise (S/N) ratio. It is smaller and its dynamic range is limited as it operates at 5 V. The Prague preamplifier is operated at 10 or 12 V and is superior in linearity and crosstalk ( $\ll 1\%$ ). However, it is larger in size and has a higher power consumption. Both preamplifiers are coupled to shapers to form the output signal. The signal of the Prague preamplifier at the output has a rise time of 40 ns and a width of 180 ns for an input signal from the APD. The corresponding values for the Minsk preamplifier are twice as large. Nine preamplifiers were placed on a printed circuit board (PCB). The bias voltage for APDs could be tuned within  $\pm 5\%$  by trimmers.

## 2.2. Signal Readout, Trigger and Data Acquisition

The analog signal output of the APDs is digitized on a 11 bit charge sensitive ADC (Le Croy 2249W) and it is eventually reduced by attenuators ( $\leq 10 \text{ dB}$ ) to match the ADC range. A CAMAC-based data acquisition is used to collect and store data. A beam trigger is provided by a coincidence of two scintillator finger counter signals. The overlapping area of the counters is  $3 \times 3 \text{ mm}^2$ . In addition to the beam, an LED and a noise trigger are produced with

a pulse generator operated at a frequency of 1 Hz. LED and a noise events are collected in between beam events. A veto signal is provided to the DAQ during the readout time to prevent event pile-up. For the APD monitoring an LED trigger allows to take specific LED signals, where the LED pulse amplitude is steerable by the driver card. The stability of the LED light pulse is monitored by a PIN diode.

## 2.3. Calibration Method

The 3 GeV  $e^+$  beam was first shot into the centre of tiles pulled out of the absorbers to get calibration factors. They account for the spread of APD gain and of properties of the optical system (scintillator, WLS, optical contacts). The contribution from a second beam particle was reduced by requiring a signal consistent with that of a minimum ionizing particle in the last layer. The calibration spectrum in each channel has been fitted with a Gaussian for the pedestal, a Gaussian for the signal peak and a Landau tail to parametrize sampling fluctuations. The distance between signal peak and pedestal position provides an ADC calibration in MIPs. Additional LED spectra were recorded for each APD channel to correct for temperature and high-voltage effects which are of order of 1 – 2% with a reproducibility of 2%. To check light uniformity in tiles, an eight-point scan around the tile center was performed in 1 cm steps which showed a 2% calibration uncertainty due to the tile inhomogeneity.

## 3. RESULTS

### 3.1. Analysis Procedure and Calibration Results

For each channel, we perform the MIP calibration described in section 2.3 and store calibration factors. Using this procedure we can measure energy of showers in units of MIPs. The calibration of showers in units of GeV can be obtained from the energy measurements in the test beam. To characterize and compare the different APD readout systems, we determine the  $S/N$  ratio, where  $S$  is the MIP amplitude and  $N \equiv \sigma_{\text{ped}}$  is the Gaussian width of the pedestal distribution. The  $S/N$  ratio is  $\approx 7$ –12 for data read out with the Minsk preamplifier and  $\approx 3$ –5 for data read out with the Prague preamplifier. Generally, the  $S/N$  ratio for data with APD readout is worse than that for readout with MAPM or SiPM (see [10]). The reason is the APD excess noise and an increased pickup noise due to a reduced intrinsic gain of APD.

The position and width of the MIP signal depend strongly on the APD working point. For example, increasing HV on APD by 5 V (at the same temperature and using Prague preamplifier), yields an enhancement of  $S/N$  by  $\approx 60$  % and  $S/\sigma_{\text{gaus}}$  by  $\approx 30$  %, respectively. Nevertheless, for our calibration procedure the results on linearity and resolution do not change.

The longitudinal shower profile for 12 layers is shown in Fig 2 for a beam energy of 5 GeV. The data (dots) are displayed in MIPs and compared to MC simulation by GEANT4. In the simulation we have accounted for various effects in the readout chain. Energy deposited in each tile is converted into photons with fluctuations represented by Poisson statistics. The number of photons is then converted into photoelectrons (pe). To match the measurements, conversions factors for ADC channels per MIP must be determined. It is done in two steps: first we calibrate ADC/pe using the MIP signal position; second we determine pe/MIP from the signal width. With this procedure a reasonable description of data is obtained for the longitudinal energy shower profile (Fig 2 shaded histogram).

### 3.2. Linearity

The energy deposited in the MiniCal in units of MIPs is summed event-by-event over all tiles. For compatibility with the SiPM results [10] the central tile of the twelfth layer was omitted. For each beam energy the resulting energy distribution is fitted with a Gaussian line shape to determine the most probable value. Figure 3 (left) shows the fit results in units of MIPs obtained for data with APD plus Minsk preamplifier (triangles) and data with APD

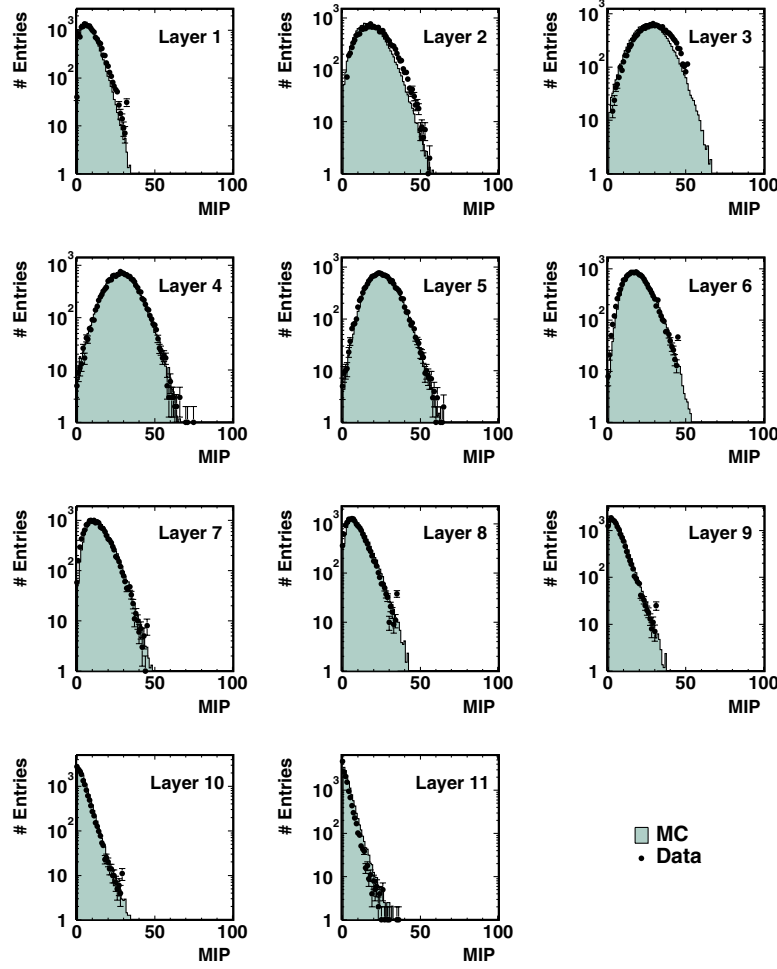


Figure 2: Longitudinal shower profile for layers 1-11 for 5 GeV  $e^+$  beam read by APDs. The shaded histogram represents MC, empty points the data. The shower profile scale is in MIPs.

plus Prague preamplifier (full points) as a function of the positron beam energy ranging from 1 GeV to 6 GeV. The Monte Carlo prediction for the MiniCal read out with APDs is shown by open points.

Assuming the calorimeter linearity a fit is performed to the data to extract the slope parameter in units of MIP/GeV. The measured energies and fitted slopes for two different preamplifiers agree at the level of 3 %, which lies within the considered systematic errors (see section 3.4). By constraining the intercept of the fit to zero changes the slope by 3 % (2 %) for data taken with the Prague (Minsk) preamplifier with respect to the unconstrained fit. The predicted values from the APD MC simulation are in good agreement with the measured results.

### 3.3. Energy Resolution

The energy resolution  $\sigma_E/E$  is derived as the spread of a signal distribution relative to the most probable signal as the function of the beam energy. The measured values for two data sets are plotted in Fig 3 (right). For comparison, the MC prediction is also shown. The stochastic terms ( $A$ ) of the energy resolution for both the Prague preamplifier and the Minsk preamplifier data, extracted from maximum likelihood fits, are in excellent agreement. In both data sets, a value of the order of 21% is obtained that agrees well with that of the APD Monte Carlo simulation. The fits are not very sensitive to the constant terms which are zero within errors. The energy resolution for the small

calorimeter prototype with APD readout in comparison to that with SiPM readout shows that the constant term in the energy resolution is insignificant and the stochastic terms are in excellent agreement. Both results are also consistent with the expectation from simulations.

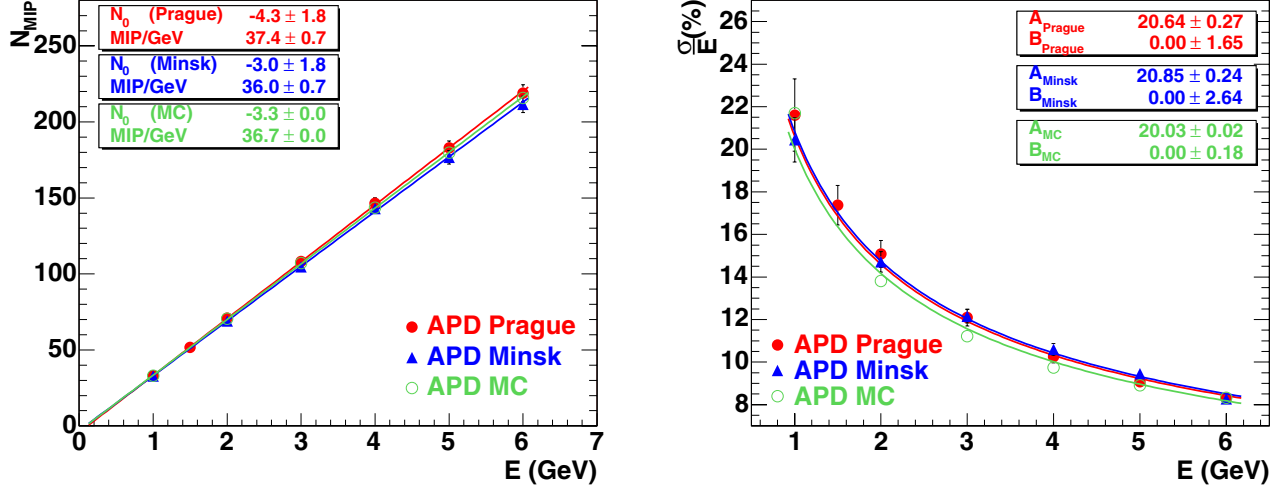


Figure 3: (left) Linearity measured with Prague (squares) and Minsk (triangles) preamplifier, respectively. Open points show MC prediction for APD measurement.

(right) Energy resolution measured with Prague (squares) and Minsk (triangles) preamplifier, respectively. Open points show the MC prediction for APD measurement. The formula  $\sigma/E(\%) = A/\sqrt{E} \oplus B$  is used for the fit to the energy resolution.

### 3.4. Systematic Errors

The errors used in the analysis include both statistical and systematic uncertainties added in quadrature. The statistical errors are typically of the order of 1.0–1.5 %. The sources of the systematic uncertainties are listed in table 3.4. The main source of systematic errors for the energy resolution measurement is electronic noise (pedestal), which contributes more significantly at low energies. The application of low-energy thresholds leads to an uncertainty  $\leq 2$  % and affects mainly low energies. Variations of conditions during calibration measurements as well as the energy scans due to temperature and high voltage adds another contribution of 3%. The nonlinearity in the energy measurement is estimated to be about 4 % at the lowest energies. Uncertainties due to the beam energy spread are of the order of 6% at 1 GeV decreasing to 2% above 3 GeV.

type	relative value	source
calibration	1 %	different calibration methods
noise	6 – 1 %	electronic noise (width of the pedestal)
thresholds	2 – 1 %	signal thresholds and cuts
stability	3 %	time stability of calibration
linearity	4 – 1 %	nonlinearity of ADC

Table I: Systematic errors of the measurements. The interval refers to an increasing energy from 1 to 6 GeV.

## 4. CONCLUSIONS

Using a positron beam with energies between 1 and 6 GeV, we have measured the linearity and resolution of a 12-layer thick calorimeter prototype as a function of energy. We have demonstrated that APDs provide an alternative option to the SiPM readout for an analog scintillating tile calorimeter. Though APDs have a gain that is about four orders of magnitude lower than that of SiPMs, and thus need a preamplifier, the MIP signal is clearly separable from the noise. Our data confirm that both a charge-sensitive and a voltage-sensitive preamplifier yield equivalent performance. The APDs do not suffer from non-linearity effects at high photon intensities. The quantum efficiency for the emission spectrum of the WLS fiber is about a factor of five higher than that for the SiPM. For stable operation a monitoring system is necessary, since gain fluctuations may occur due to temperature changes and high voltage fluctuations. The present study shows that these variations can be reliably corrected for. The linearity for APD readout with both preamplifier designs is in good agreement. The sampling fluctuations in the shower development are sufficiently large that the difference in noise performance of the two preamplifiers is insignificant. The energy resolution we have measured with APD readout is in excellent agreement with that obtained for SiPM readout.

## Acknowledgments

The results presented here were done in the collaboration with my colleagues E. Devitsin, V. Dodonov, G. Eigen, E. Garutti, Yu. Gilitski, M. Groll, M. Janata, I. Kacł, V. Korbel, H. Meyer, V. Morgunov, S. Němeček, R. Pöschl, I. Polák, E. Popova, A. Raspereza, S. Reiche, E. Sefkow, P. Smirnov, Š. Valkár, J. Weichert and J. Zálešák.

This work is supported by the contribution of Bundesministerium für Bildung und Forschung, Germany; Alexander von Humboldt Foundation (Research Award IV, RUS 1066839 GSA), INTAS (Grant # YSF150-00); the Russian grants SS551722.2003.2 and RFBR0402/17307a; the Ministry of Education of the Czech Republic under the project LC527 and INGO-1P05LA259 and by the Grant Agency of the Czech Republic under the project 202/05/0653.

## References

- [1] Memorandum to the PRC, from the proposal 01/02, DESY, Hamburg, Memo-01, CALICE collaboration, October 2001, [http://polywww.in2p3.fr/flc/calice\\_offic.html](http://polywww.in2p3.fr/flc/calice_offic.html).
- [2] TESLA TDR, DESY 2001-011 (2001).
- [3] H. Videau, J.-C. Brient, Calorimetry Optimized for Jets, *Proceedings of the 10<sup>th</sup> International Conference on Calorimetry in Particle Physics*, Pasadena, March 2002, World Scientific 2002, p. 747.
- [4] V. Morgunov, Calorimeter Design in the Energy Flow Concept, *Proceedings of the 10<sup>th</sup> International Conference on Calorimetry in Particle Physics*, Pasadena, March 2002, World Scientific 2002, p. 70.
- [5] F. Sefkow, Performance Goals and Design Considerations for a Linear Collider Calorimeter, *Proceedings of the 11<sup>th</sup> Int. Conf. on Calorimetry in Particle Physics*, Perugia, March 2004, World Scientific 2005, p. 435.
- [6] J. Cvach, Calorimetry at a Future  $e^+e^-$  Collider, *Proceedings of ICHEP 2002, Amsterdam*, Elsevier Science B.V. 2003, p. 922.
- [7] V. Korbel, A Scintillator Tile Hadron Calorimeter for the Linear Collider Detector, *Proc. of 9th Topical Seminar on Innovative Particle and Radiation Detectors*, Siena (2004).
- [8] G. Bondarenko et al., Nucl. Instrum. Meth. A **442** (2000) 187.
- [9] V. Andreev et al., A High-Granularity Plastic Scintillator Tile Hadronic Calorimeter with APD Readout for a linear Collider Detector, to be published in NIM A.
- [10] V. Andreev et al., Nucl. Instr. Meth. A **540** (2005) 368.
- [11] H. Meyer, Diploma Thesis, University of Hamburg 2004.